analytical chemistry

ARTICLE

pubs.acs.org/ac

Semi-Infinite Linear Diffusion Spectroelectrochemistry on an Aqueous *Micro*-Drop

Cynthia A. Schroll,[†] Sayandev Chatterjee,[‡] William R. Heineman,[*,†] and Samuel A. Bryan[*,‡]

[†]Department of Chemistry, University of Cincinnati, Cincinnati, Ohio 45221-0172, United States

[‡]Energy and Environment Directorate, Pacific Northwest National Laboratory, Richland, Washington 99352, United States

ABSTRACT: We report a technique for conducting semi-infinite diffusion spectroelectrochemistry on an aqueous *micro*-drop as an easy and economic way of investigating spectroelectrochemical behavior of redox active compounds and correlating spectroscopic properties with thermodynamic potentials on a small scale. The chemical systems used to demonstrate the aqueous *micro*-drop technique were an absorbance based ionic probe $[Fe(CN)_6]^{3-/4-}$ and an emission based ionic probe $[Re(dmpe)_3]^{2+/+}$. These chemical systems in a *micro*-drop were evaluated using cyclic voltammetry and UV−visible absorbance and luminescence spectroscopies.

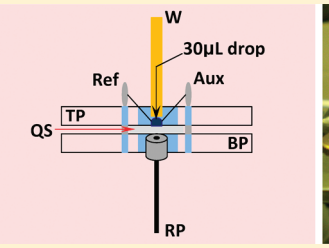

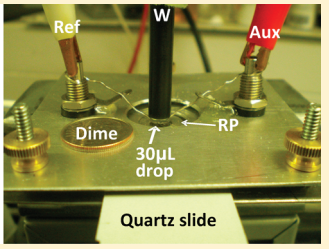

Over the past several decades spectroelectrochemistry has gained importance as a technique for measuring the redox[1] and spectral properties of inorganic,[2−7] organic,[6,8,9] and biological[10−13] species. Spectroelectrochemistry can be implemented in cells that are characterized by either semi-infinite linear diffusion (SILD) in a bulk solution or by thin layer cells in which complete electrolysis is rapidly achieved in a thin layer of solution with restricted diffusion. The spectroscopic methods that have been used rely on light propagation through the sample based on transmission, specular reflection, or internal reflection.[14] In transmission spectroscopy the light beam is passed through an optically transparent electrode and the sample.[1,15−17] In specular reflection spectroscopy the light is passed through the sample, reflected off the electrode surface, and then passed back through the sample.[18−21] In internal reflection spectroscopy the light is directed into a waveguide at an angle greater than the critical angle so that it is internally reflected. At each reflection point an evanescent electromagnetic wave interacts with the sample, and the changes in the spectra can be measured.[22,23]

SILD spectroelectrochemistry has been used for a wide range of applications.[24−27] In spite of the broad scope of SILD spectroelectrochemistry, wide applicability of the technique is limited by cell designs that are complicated to construct and use and which require relatively large sample sizes—on the order of milliliters.[15,25,28,29] Cell designs that have the working electrode positioned so that either thin-layer or SILD spectroelectrochemistry can be achieved on a smaller volume of sample have been reported.[30−32]

In an effort to substantially reduce the sample size and the cell complexity of the SILD cell without compromising a rapid experimental execution time, we herein describe a technique of *micro*-drop spectroelectrochemical detection based on a modification of a method reported by Wijayawardhana et al.[33] This group used a rotating disk electrode (RDE) for electrochemical immunoassay on a 50 μL drop sandwiched between the RDE and an inert bottom plate, with the reference and auxiliary electrodes inserted into the drop from the side. Our aim is to couple this electrochemical technique with simultaneous spectroscopic detection to acquire spectroelectrochemical data in an easy and rapid way and to keep the total sample volume as small as possible.

This technique would be useful for studying spectroelectrochemical processes where minimizing sample size is critically important because of expense, limited supply, or waste disposal issues as with radioactive compounds. This work was stimulated by our particular interest to do spectroelectrochemistry in ionic liquid solutions of actinides and other radioactive materials and waste forms where all of these issues apply.

EXPERIMENTAL SECTION

Chemicals and Materials. Potassium ferricyanide ($K_3[Fe(CN)_6]$), sodium ferrocyanide ($Na_4[Fe(CN)_6]$), and potassium nitrate (KNO_3) were obtained from Sigma-Aldrich and used without further purification. *Tris*-(*bis*-(1,2-dimethylphosphinoethyl))-rhenium(I) triflate ($[Re(dmpe)_3](OTf)$) was synthesized via a literature method.[34] Aqueous solutions of $K_3[Fe(CN)_6]$, $Na_4[Fe(CN)_6]$, and $[Re(dmpe)_3](OTf)$ were made by dissolving the appropriate amount of reagent in 0.1 M KNO_3 solution. To make the glass slide's surface hydrophobic it was siliconized with Surfasil (Pierce Chemical Co.). Siliconization was done to ensure the formation of a spherical drop to allow a sufficiently large distance between the electrode surface and the glass slide to have semi-infinite diffusion on the time scale of a typical scan time for cyclic voltammetry.

Received: March 2, 2011
Accepted: April 16, 2011
Published: April 17, 2011

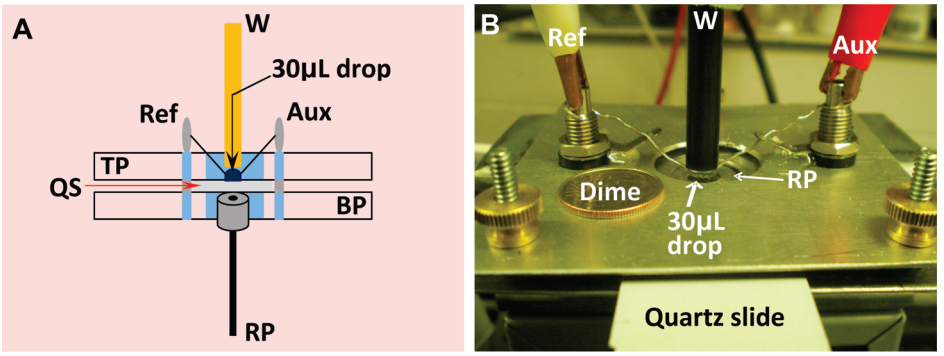

Figure 1. (A) Schematic representation of the spectroelectrochemical setup using an aqueous *micro*-drop, (B) a photograph of the cell. (W = working electrode, ref = reference electrode, Aux = auxiliary electrode, TP = top plate, QS = quartz slide, BP = bottom plate, RP = reflectance probe).

Instrumentation. Cyclic voltammetry on the aqueous *micro*-drop was carried out using an Epsilon Potentiostat (Bioanalytical Systems) with a standard three-electrode cell stand from Bioanalytical Systems. All scans were recorded using a glassy carbon working electrode (area 7.07 mm^2) and a Pt wire auxiliary electrode. Between measurements, the working electrode was polished with 0.05 μm alumina slurry and a polishing pad, rinsed with distilled water, and wiped dry using a Kimwipe. All reported potentials are referenced versus a platinum wire quasi-reference electrode. Peak currents (i_p) were measured with respect to the extrapolated baseline current as described by Kissinger and Heineman.[35] UV−visible absorption spectra were recorded with a deuterium light source (Mikropack, model# DH 2000) and an Ocean Optics USB2000 detector (188−880 nm) using Spectra Suite Software for spectral data acquisitions. Emission spectra were recorded using a 532 nm laser excitation source (Melles Griot, 20 mW CW), coupled to an InSpectrum 150 spectrometer-CCD, and using SpectraSense data acquisition software. A 532 nm holographic notch filter (Kaiser) was used to reduce laser light backscattered into the InSpectrum 150 spectrometer. Signal integration times were typically 500 ms using a 2-mm slit width for a 600 gr/mm grating blazed at 500 nm. Step-index silica-on-silica optical fibers were purchased from Romack, Inc. The Ocean Optics system consisted of a USB-200FL spectrometer and Ocean Optics 00IBase32 Spectroscopy Software.

In a typical setup as illustrated in Figure 1, a glass slide was placed on a stand above the reflectance probe. The custom designed stand consisted of two aluminum plates separated by an O-ring spacer to allow an optically transparent surface (e.g., quartz plate or glass microscope slide) to slide in. A hole was drilled at the center of the aluminum plates to permit passage of the optical beam. The upper aluminum plate was held in place with thumb screws that also provided conducting surfaces to attach the reference and working electrodes. The auxiliary and reference wire electrodes were spaced approximately 1 mm apart from one another. To ensure that the electrodes were relatively immobile during the entire course of the experiment, they were glued to the posts with epoxy resin. This limited the free mobility of the reference and the auxiliary electrodes, and preserved the relative distance, alignment, and orientation between the individual electrodes. The working electrode was lowered to within ~1 mm from the glass surface, and a 30 μL drop of solution was placed in between. The distance of the tip of the working electrode from the glass surface was set at 1 mm (which equals half the total optical path length) using slide calipers. The path length determined from the absorbance at 420 nm of a microdrop of a solution containing a known concentration of $K_3Fe(CN)_6$, confirmed the distance to within 5% of experimental error. The drop was positioned to cover the reference and auxiliary electrodes while surface tension ensured its contact with the working electrode from above. A 180° back-reflectance UV−visible-NIR probe with a bundle of fiber-optic cables was fixed to a clamp directly below the glass slide surface for spectral measurement and focused directly on the surface of the working electrode. The reflectance probe configuration was six peripheral fiber optic cables for excitation coming from the light source, with one concentrically located cable for collection of the light transmitted after reflection from the surface of the disk working electrode, going to the detector.

RESULTS AND DISCUSSION

To explore this technique, two model compounds with known electrochemical and spectroscopic properties were chosen. The chemical systems used to demonstrate the *micro*-drop technique were an absorbance based ionic probe $[Fe(CN)_6]^{3-/4-}$ and a luminescence based ionic probe $[Re(dmpe)_3]^{2+/+}$. Both systems are characterized by a chemically reversible electrochemical couple and demonstrate the general requirements of absorbance and luminescence based systems, respectively.

$[Fe(CN)_6]^{3-}$/$[Fe(CN)_6]^{4-}$ System. For absorbance experiments, the $[Fe(CN)_6]^{3-}/[Fe(CN)_6]^{4-}$ couple ($E^{o\prime}$ = 0.25 V vs Ag/AgCl) was chosen. The two redox forms are spectroscopically distinguishable; an aqueous solution of $[Fe(CN)_6]^{4-}$ (pH = 7, T = 25 °C) is optically transparent at 420 nm while $[Fe(CN)_6]^{3-}$ has a strong absorption band at this wavelength under identical conditions (ε_{420} = 1040 M^{-1} cm^{-1}).[36] Thus, oxidation of Fe(II) to Fe(III) results in the appearance of the 420 nm band, while the reduction of $[Fe(CN)_6]^{3-}$ back to $[Fe(CN)_6]^{4-}$ results in a decrease in its intensity.

Cyclic Voltammetry of $[Fe(CN)_6]^{3-}$/$[Fe(CN)_6]^{4-}$. Cyclic voltammetry was used to evaluate the electrochemical properties of the cell, measure $E^{o\prime}$, and determine the diffusion coefficients of the $[Fe(CN)_6]^{3-}/[Fe(CN)_6]^{4-}$ system. The $E^{o\prime}$ for this redox process was −0.1 V vs the quasi-reference electrode for all scans with a ΔE_p = 120 mV (ν = 50 mV s^{-1}). This ΔE_p is larger than the expected 59 mV for an electrochemically reversible $1e^-$ system and is attributed to the slow electron transfer that can occur at glassy carbon. Cyclic voltammograms of 5.0 mM $K_3[Fe(CN)_6]$ in 0.1 M KNO_3 solution as a function of scan rate

dx.doi.org/10.1021/ac200551n |*Anal. Chem.* 2011, 83, 4214–4219

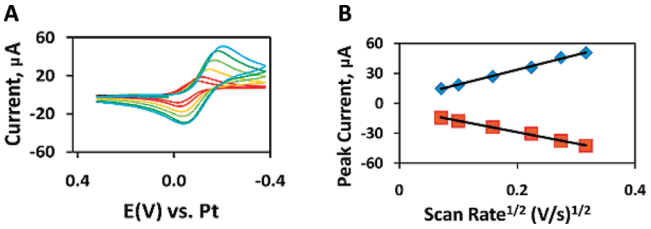

Figure 2. (A) Cyclic voltammograms of an aqueous solution of 5.0×10^{-3} M $K_3[Fe(CN)_6]$, 0.1 M KNO_3 as a function of scan rate, (light brown line) 5, (red line) 10, (yellow line)) 25, (light green line) 50, (green line) 75, and (light blue line) 100 mV/s (GC disk working electrode, Pt wire reference electrode and Pt wire auxiliary electrode). (B) Plot of peak current versus the square root of scan rate: (solid light brown squares) anodic wave; $i_{pa}(\mu A) = -114\,\nu^{1/2}\,(V\,s^{-1})^{1/2} - 6.1$ (R^2 = 0.997); (solid blue diamonds) cathodic wave; $i_{pc}(\mu A) = 149\,\nu^{1/2}\,(V\,s^{-1})^{1/2} + 3.9$ (R^2 = 0.997).

(Figure 2A) have voltammograms that are consistent with semi-infinite diffusion for scan rates ranging from 5 to100 mV s^{-1}.[37] The positive shift in the potential of both the reduction and the oxidation peaks is due to the change in concentration of the oxidative and reductive species with respect to the Pt quasi-reference electrode. This was further confirmed by a control experiment where the cyclic voltammetry of a 5.0 mM $K_3[Fe(CN)_6]$ in 0.1 M KNO_3 solution in a standard cell referenced to a Pt quasi reference electrode was compared to that using a Ag/AgCl reference electrode. The potential for both peaks again shifted in a positive direction when the Ag/AgCl reference electrode was replaced by the Pt quasi reference.

A plot of peak currents versus the square root of scan rates (Figure 2B) is linear as expected for semi-infinite diffusion. Using the Randle−Sevcik equation[35] the diffusion coefficient for $[Fe(CN)_6]^{3-}$ was found to be 2.4×10^{-6} cm^2 s^{-1} which is in agreement with the literature.[38] The peak current ratio of i_p/i_c = 0.76 indicates that the $[Fe(CN)_6]^{3-}/[Fe(CN)_6]^{4-}$ redox couple is quasi-reversible. The quasi-reversibility is indicative of adsorption of analyte to the surface of the glassy carbon from the solution.[39] The performance is very similar to that obtained using a glassy carbon working electrode in a conventional regular volume three component electrochemical cell setup and confirms the semi-infinite linear diffusion, even at slower scan rates.

Chronoabsorptometry of $[Fe(CN)_6]^{3-}/[Fe(CN)_6]^{4-}$. Double potential step chronoabsorptometry was used to evaluate the spectroelectrochemical characteristics of the cell. In a typical experiment, a forward step of 0.4 V was applied to an aqueous solution of 25 mM $[Fe(CN)_6]^{4-}$, 0.1 M KNO_3 for 90 s while absorption spectra were concurrently recorded at 5 s intervals. The oxidation of $[Fe(CN)_6]^{4-}$ to $[Fe(CN)_6]^{3-}$ was characterized by the appearance and growth of the 420 nm absorption band. Subsequently, the reverse step to −0.4 V for 90 s resulted in a decrease in intensity of this absorption band, demonstrating a reduction of $[Fe(CN)_6]^{3-}$ back to $[Fe(CN)_6]^{4-}$. A plot of absorbance versus time at 420 nm for both forward and reverse potential steps is shown in Figure 3A. It can be seen that the system levels off to a maximum absorbance within 40 s from the start of the oxidation while a minimum value is reached within 40 s of the start of the back reduction. Using the equation:

$$\delta = (2Dt)^{1/2} \qquad (1)$$

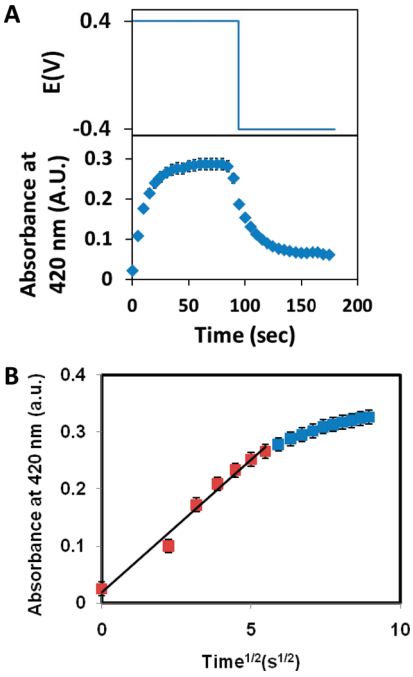

Figure 3. (A) Double potential step chronoabsorptometry at 420 nm of an aqueous solution of 25.0×10^{-3} M $Na_4[Fe(CN)_6]$, 0.1 M KNO_3 (Glassy carbon working electrode, Pt wire reference electrode and Pt wire auxiliary electrode). A potential of 0.4 V applied for 90 s resulted in an increase and subsequent leveling off in absorbance. An immediate subsequent application of −0.4 V resulted in a decrease followed by subsequent leveling off of the absorbance. (B) Plot of Absorbance vs $Time^{1/2}$, for the oxidation step. The red squares represent the diffusion controlled region, while the blue squares represent the deviation. The equation for the diffusion controlled region is $A(a.u.) = 0.047\,t^{1/2}(s^{1/2}) + 0.02$ (R^2 = 0.98). The standard errors for the slope and intercept are (+0.002, −0.007) and (±0.006), respectively.

where δ is the Nernst diffusion layer, D is the diffusion coefficient of ferrocyanide, and t is time, it is calculated that the electrolysis should take about 60 min. This calculated time for complete electrolysis confirms that under our experimental parameters, where each potential was held for less than 2 min, only a small fraction of the total volume of the working solution was electrolyzed, and semi-infinite diffusion conditions existed.

Thus, the leveling off of absorbance in the forward step of Figure 3A is not due to complete electrolysis of the absorbing species, but rather is attributed to the optical configuration of the cell. The reflectance probe surface, composed of a fiber bundle 2 mm in diameter, illuminates the glassy carbon electrode (GCE), whose surface area is 3 mm in diameter, located a distance of 1 mm away from each other. At this distance, the reflectance probe beam divergence is larger than the active area of the GCE, and under the existing experimental settings, the spectroscopically interrogated solution volume includes solution outside of the diffusion layer adjacent to the GCE. Under these conditions, Beer's Law behavior will not strictly be observed, which explains why the change in absorbance in Figure 3A levels off more rapidly than otherwise would be predicted. Using a larger electrode surface area or a more collimated beam would reduce this effect. Additionally, by continuing the measurement for longer than 5 min the gradual evaporation of the drop was observed, as evidenced by an increase in the absorbance intensity of the plateau even while holding the potential of the working electrode at −0.4 V.

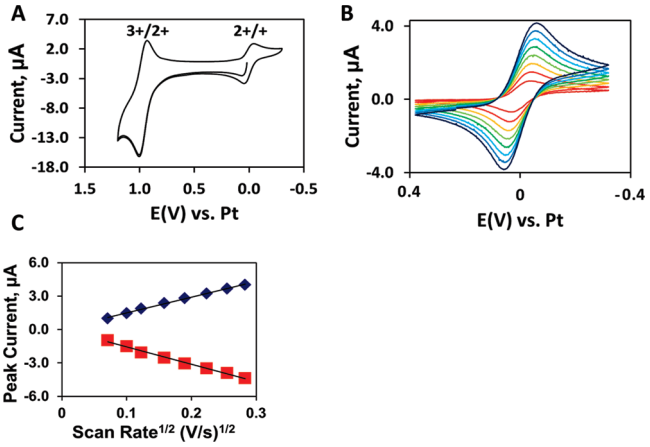

Figure 4. (A) Cyclic voltammogram of an aqueous solution of 1.25×10^{-3} M $[Re(dmpe)_3](OTf)$, 0.1 M KNO_3 at $\nu = 50$ mV s^{-1} showing the two redox couples of $Re(dmpe)_3(OTf)$. (B) Cyclic voltammograms of an aqueous solution of 1.25×10^{-3} M $Re(dmpe)_3(OTf)$, 0.1 M KNO_3 as a function of scan rate, (light brown line) 5, (red line) 10, (yellow line) 15, (light green line) 25, (green line) 36, (light blue line) 50, (blue line) 65, and (dark blue line) 80 mV/s (Glassy carbon working electrode, Pt wire reference electrode and Pt wire auxiliary electrode). (C) Plot of peak current versus the square root of scan rate: (solid red squares) anodic process for $[Re(dmpe)_3]^{2+}/[Re(dmpe)_3]^{+}$; i_{pa} (μA) = −15.6 $\nu^{1/2}$ (V $s^{-1})^{1/2}$ − 0.8 (R^2 = 0.997); (solid blue diamonds) cathodic process for $[Re(dmpe)_3]^{2+}/[Re(dmpe)_3]^{+}$; i_{pc} (μA) = 14.1 $\nu^{1/2}$ (V $s^{-1})^{1/2}$ + 0.005 (R^2 = 0.994).

A plot of absorbance versus the square root of time for the oxidation process is shown in Figure 3B. From this plot it can be seen that the absorbance change starts as a diffusion controlled system, but at approximately 40 s there is a deviation from the diffusion controlled system for the reasons discussed above. Applying the equation for chronoabsorptometry to the slope of the linear portion of the graph (Figure 3B) that adheres to Beer's Law:

$$A = \frac{2\varepsilon_0 D^{1/2} C t^{1/2}}{\pi^{1/2}} \qquad (2)$$

where A is the absorbance, ε_o is the molar absorptivity of ferricyanide, D is defined from eq 1, C is the concentration of ferrocyanide, and t is time; the molar absorptivity of ferricyanide was calculated be $\varepsilon_{420\ nm}$ = 1390 M^{-1} cm^{-1}.[40,41] This is similar to the accepted value of 1100 M^{-1} cm^{-1}[42] and confirms the semi-infinite diffusion conditions.

$[Re(dmpe)_3]^{2+}/[Re(dmpe)_3]^{+}$ System. For emission experiments, $[Re(dmpe)_3](OTf)$ was chosen to take advantage of the changes in luminescence properties of the complex associated with the reversible $[Re(dmpe)_3]^{2+/+}$ ($E^{o\prime}$= 0.34 V vs Ag/AgCl) redox couple. $[Re(dmpe)_3]^{2+}$ emits at 605 nm (λ_{ex} = 532 nm) while $[Re(dmpe)_3]^{+}$ does not emit at this wavelength.[43] The complex has also been reported to exhibit a second redox process ($E^{o\prime}$ = 1.12 V vs Ag/AgCl; chemically quasi-reversible as determined by the ratio of the peak currents) assigned to the $Re^{3+/2+}$ couple.

Cyclic Voltammetry of $[Re(dmpe)_3]^{2+}/[Re(dmpe)_3]^{+}$. Cyclic voltammetry was used to determine the $E^{o\prime}$ of both the $[Re(dmpe)_3]^{2+}/[Re(dmpe)_3]^{+}$ and $[Re(dmpe)_3]^{3+}/[Re(dmpe)_3]^{2+}$ couples as well as the diffusion coefficients for $[Re(dmpe)_3]^{2+}$ and $[Re(dmpe)_3]^{+}$. The cyclic voltammograms of the complex within the potential range 1.2 V and −0.3 V shows the two redox processes (Figure 4A). The lower potential process ($E^{o\prime}$ = 0.002 V; ΔE_p = 87 mV) is assigned to the $[Re(dmpe)_3]^{2+}/[Re(dmpe)_3]^{+}$ couple while the higher potential process ($E^{o\prime}$ = 0.97 V; ΔE_p = 71 mV) is assigned to the $Re^{3+/2+}$ couple . Cyclic voltammograms as a function of scan rate for the $[Re(dmpe)_3]^{2+}/[Re(dmpe)_3]^{+}$ couple (Figure 4B) have voltammograms that are consistent with semi-infinite diffusion for scan rates from 5 to 80 mV s^{-1}.[43] As expected, the increase in peak current is directly related to the increase in the square root of scan rate (Figure 4C). The ratio of the slope of the peak currents as a function of square root of scan rate for the $[Re(dmpe)_3]^{2+}/[Re(dmpe)_3]^{+}$ couple is calculated to be i_p/i_c = 0.90. It was expected that the i_p/i_c would be less than one because of the air oxidation of $[Re(dmpe)_3]^{+}$ to $[Re(dmpe)_3]^{2+}$. Furthermore, a Randle−Sevcik analysis[35] showed that $[Re(dmpe)_3]^{+}$ has a diffusion coefficient of 4.34×10^{-7} cm^2 s^{-1}. The diffusion coefficient of $[Re(dmpe)_3]^{2+}$ during its reduction to $[Re(dmpe)_3]^{+}$ is 3.53×10^{-7} cm^2 s^{-1}. This performance is close to that obtained for a glassy carbon electrode dipped into a conventional electrochemical cell confirming semi-infinite diffusion, even at the slower scan rates. Because of significantly reduced chemical reversibility and significantly less pronounced changes in the spectroscopic properties, the $[Re(dmpe)_3]^{3+}/[Re(dmpe)_3]^{2+}$couple was not further explored for the purpose of this paper.

Luminescence Based Spectroelectrochemistry of $[Re(dmpe)_3]^{2+}/[Re(dmpe)_3]^{+}$. The cell's capacity for luminescence based spectroelectrochemistry was demonstrated using the $[Re(dmpe)_3]^{2+}/[Re(dmpe)_3]^{+}$ couple. Since $[Re(dmpe)_3]^{+}$ air oxidizes to $[Re(dmpe)_3]^{2+}$, a water-saturated N_2 blanket was placed over the working electrode assembly. A potential of 0.4 V was applied to an aqueous solution of 1.25 mM $[Re(dmpe)_3](OTf)$, 0.1 M KNO_3 for 90 s, and a series of luminescence spectra were recorded at 10 s intervals under 532 nm laser excitation. The oxidation of $[Re(dmpe)_3]^{+}$ to $[Re(dmpe)_3]^{2+}$ was characterized by the appearance and growth of the 605 nm emission band. An immediate change in potential to −0.6 V for 90 s resulted in a decrease in intensity of the 605 nm emission band, indicating reduction of $[Re(dmpe)_3]^{2+}$ back to the starting material, $[Re(dmpe)_3]^{+}$ (Figure 5A).

The profile of the emission maximum is shown in the time versus 605 nm emission intensity plot (Figure 5B). Modulation of luminescence intensity at 605 nm by sequential application of a positive potential (0.4 V) for 120 s, followed by immediate application of a negative potential (−0.6 V) repeated for two cycles, showed a sinusoidal behavior in the intensity. The baseline slope (the line formed by extrapolation through the local intensity minima) showed a positive slope of 1.3. A control experiment conducted in which luminescence intensity of an aqueous solution of 1.25 mM $[Re(dmpe)_3](OTf)$, 0.1 M KNO_3 was monitored under excitation by the same 532 nm laser source in the absence of any potential exhibited a similar slope (1.5), indicating the slope in the modulated curve is due to aerial oxidation. Figure 5B shows the intensity vs time for the control run, illustrating that in the absence of an applied potential, there is a gradual appearance of the 605 nm emission band. We are currently working on modifications to reduce exposure to atmosphere to limit the chemical oxidation of air sensitive analytes. Shown in Figure 5C is a plot of luminescence vs $time^{1/2}$ for the first oxidation of $[Re(dmpe)_3]^{+}$. The linear plot confirms semi-infinite diffusion throughout the step.

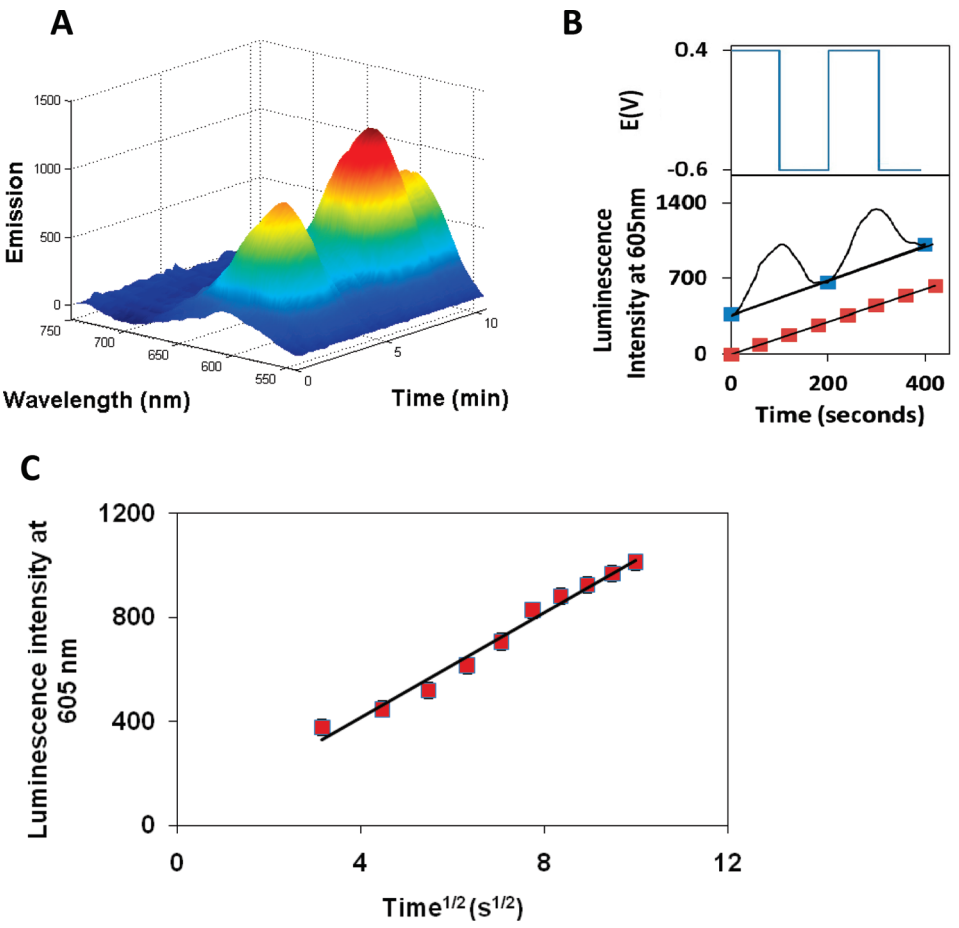

Figure 5. (A) Modulation of luminescence intensity of an aqueous solution 1.25×10^{-3} M $[Re(dmpe)_3](OTf)$, 0.1 M KNO_3 with time on the application of voltage (λ_{ex} = 532 nm). A potential of 0.4 V applied for 120 s resulted in an increase and subsequent leveling off in intensity. An immediate subsequent application of −0.6 V for 120 s resulted in a decrease followed by subsequent leveling off of the intensity. This process was repeated for two cycles. (B) Modulation of luminescence intensity at 605 nm: (solid blue squares) Points at the trough of each modulation where there is a maximum concentration of $[Re(dmpe)]^+$ present. The equation of the line passing through the troughs is I(a.u.) = 1.60t(s) + 360. (solid light bown squares) Control run of solution 1.25×10^{-3} M $[Re(dmpe)_3](OTf)$, 0.1 M KNO_3 where no voltage was applied. The equation of the line is I(a.u.) = 1.50t(s) . (C) Plot of Luminescence vs Time$^{1/2}$ for the oxidation of 1.25×10^{-3} M $[Re(dmpe)_3](OTf)$, 0.1 M KNO_3. The equation of the line is I(a.u.) = 101$t^{1/2}$(s$^{1/2}$) + 9 (R^2 = 0.98). The standard errors for the slope and intercept are (+ 1, −6) and (± 10), respectively.

CONCLUSIONS

SILD spectroelectrochemistry using either absorption or emission spectroscopy can be done on a 30 μL drop of liquid with a cell that is easy to fabricate and use. SILD conditions were maintained over the time scale corresponding to cyclic voltammetry scan rates as slow as 2 mV s^{-1}. Optical sensitivity was sufficient to easily monitor absorbance and fluorescence changes associated with the electrochemistry. The cell has the advantage of not requiring electrode transparency, making it more widely applicable than spectroelectrochemical techniques in which optical measurements are made through the electrode. The cell could be easily converted into a thin layer cell by simply reducing the distance between the electrode and the bottom plate. Improvements that could be made include enlarging the electrode surface or reducing the optical beam so that only the diffusion layer is monitored and provision for deoxygenation. The effectiveness and reproducibility of this method for studying spectroelectrochemical processes in microquantities of analyte makes the technique promising for substances that are expensive, limited in available quantity, or pose disposal issues because of toxicity or radioactivity.

AUTHOR INFORMATION

Corresponding Author

*E-mail: sam.bryan@pnl.gov (S.A.B.), heinemwr@ucmail.uc.edu (W.R.H.).

ACKNOWLEDGMENT

This research was supported by the U.S. Department of Energy's Fuel Cycle Research and Development (FCR&D), Separation Campaign (NE) and performed at the Pacific Northwest National Laboratory operated by Battelle for the U.S. Department of Energy under Contract DE-AC05-76RL01830. Support from the Office of Science, BER (Grant No. DE-FG02-07ER64353), and the Office of Environmental Management Sciences Program (Grant No. DE-FG0799ER62331) of the U.S. Department of Energy (DOE) is also gratefully acknowledged. We thank Dr. Necati Kaval for designing the InSpectrum 150 spectrometer-CCD, Eme Amba Abu for helpful discussions, and Amos Doepke for preparing the hydrophobic glass slides.

REFERENCES

(1) Kuwana, T.; Darlington, R. K.; Leedy, D. W. *Anal. Chem.* **1964**, *36*, 2023.
(2) Rieder, K.; Hauser, U.; Siegenthaler, H.; Schmidt, E.; Ludi, A. *Inorg. Chem.* **1975**, *14*, 1902.
(3) Rohrbach, D. F.; Heineman, W. R.; Deutsch, E. *Inorg. Chem.* **1979**, *18*, 2536.
(4) Hill, M. G.; Penneau, J. F.; Zinger, B.; Mann, K. R.; Miller, L. L. *Chem. Mater.* **1992**, *4*, 1106.
(5) Kaim, W.; Klein, A.; Hasenzahl, S.; Stoll, H.; Zalis, S.; Fiedler, J. *Organometallics* **1998**, *17*, 237.
(6) Toma, H. E.; Araki, K. *Curr. Org. Chem.* **2002**, *6*, 21.
(7) Lahiri, G. K.; Kaim, W. *Dalton Trans.* **2010**, *39*, 4471.
(8) Owens, J. L.; Marsh, H. A.; Dryhurst, G. *J. Electroanal. Chem.* **1978**, *91*, 231.
(9) Stutts, K. J.; Powell, L. A.; Wightman, R. M. *J. Electrochem. Soc.* **1981**, *128*, 1248.
(10) Heineman, W. R.; Norris, B. J.; Goelz, J. F. *Anal. Chem.* **1975**, *47*, 79.
(11) Sailasuta, N.; Anson, F. C.; Gray, H. B. *J. Am. Chem. Soc.* **1979**, *101*, 455.
(12) Larsson, T.; Lindgren, A.; Ruzgas, T. *Bioelectrochemistry* **2001**, *53*, 243.
(13) Comtat, M.; Durliat, H. *Biosens. Bioelectron.* **1994**, *9*, 663.
(14) Heineman, W. R. *Anal. Chem.* **1978**, *50*, 390A.
(15) Strojek, J. W.; Kuwana, T. *J. Electroanal. Chem.* **1968**, *16*, 471.
(16) Kuwana, T.; Strojek, J. W. *Faraday Discuss.* **1968**, *45*, 134.
(17) Osa, T.; Kuwana, T. *J. Electroanal. Chem.* **1969**, *22*, 389.
(18) Bewick, A.; Tuxford, A. M. *Symp. Faraday. Soc.* **1970**, *4*, 114.
(19) Aylmer-Kelly, A. W. B.; Bewick, A.; Cantrill, P. R.; Tuxford, A. M. *Faraday Discuss.* **1973**, *56*, 96.
(20) Pruiksma, R. *J. Electroanal. Chem.* **1980**, *114*, 147.
(21) Gaillard, F.; Levillain, E. *J. Electroanal. Chem.* **1995**, *398*, 77.
(22) Hansen, W. N.; Kuwana, T.; Osteryoung, R. A. *Anal. Chem.* **1966**, *38*, 1810.
(23) Prostak, A.; Mark, H. B.; Hansen, W. N. *J. Phys. Chem.* **1968**, *72*, 2576.
(24) Kuwana, T.; Heineman, W. R. *Acc. Chem. Res.* **1976**, *9*, 241.
(25) Kuwana, T.; Winograd, N. In *Electroanalytical Chemistry*; Bard, A. J., Ed.; Marcel Dekker: New York, 1974; p 1.
(26) Heineman, W. R.; Hawkridge, F. M.; Blount, H. N. In *Electroanalytical Chemistry*; Bard, A. J., Ed.; Marcel Dekker: New York, 1984; p 1.
(27) Niu, J.; Dong, S. *Rev. Anal. Chem.* **1996**, *15*, 1.
(28) Winograd, N.; Kuwana, T. *J. Electroanal. Chem.* **1969**, *23*, 333.
(29) Winograd, N.; Kuwana, T. *Anal. Chem.* **1971**, *43*, 252.
(30) Porter, M. D.; Dong, S. J.; Gui, Y. P.; Kuwana, T. *Anal. Chem.* **1984**, *56*, 2263.
(31) Salbeck, J. *J. Electroanal. Chem.* **1992**, *340*, 169.
(32) Heineman, W. R.; Kuwana, T. *Anal. Chem.* **1972**, *44*, 1972.
(33) Wijayawardhana, C. A.; Halsall, H. B.; Heineman, W. R. *Anal. Chim. Acta* **1999**, *399*, 3.
(34) Deutsch, E.; Libson, K.; Vanderheyden, J. L.; Ketring, A. R.; Maxon, H. R. *Int. J. Radiat. Appl. Instrum. B* **1986**, *13*, 465.
(35) Kissinger, P. T.; Heineman, W. R. *J. Chem. Educ.* **1983**, *60*, 702.
(36) Krenitsky, T. A.; Neil, S. M.; Elion, G. B.; Hitchings, G. H. *Arch. Biochem. Biophys.* **1972**, *150*, 585.
(37) Bard, A. J.; Faulkner, L. R. *Electrochemical Methods: Fundamentals and Applications*, 2nd ed; Wiley: New York, 2001; p 147.
(38) Konopka, S. J.; McDuffie, B. *Anal. Chem.* **1970**, *42*, 1741.
(39) Yang, R.; Qian, Z.; Deng, J. *J. Electrochem. Soc.* **1998**, *145*, 2231.
(40) Ogura, K.; Naito, T. *Electrochim. Acta* **1982**, *27*, 1243.
(41) Bard, A. J.; Faulkner, L. R. *Electrochemical Methods: Fundamentals and Application*, 2 ed.; Wiley: New York, 2001; p 682.
(42) Alexander, J. J.; Gray, H. B. *J. Am. Chem. Soc.* **1968**, *90*, 4260.
(43) Kirchhoff, J. R.; Allen, M. R.; Cheesman, B. V.; Okamoto, K.; Heineman, W. R.; Deutsch, E. *Inorg. Chim. Acta* **1997**, *262*, 195.